Knowl. Manag. Aquat. Ecosyst. 2025, 426, 26 © G. Exley *et al.*, Published by EDP Sciences 2025 https://doi.org/10.1051/kmae/2025021

www.kmae-journal.org

Knowledge & Management of Aquatic Ecosystems

Journal fully supported by Office français de la biodiversité

Research Paper Open 3 Access

Modelling of the potential of floating photovoltaics for mitigating climate change impacts on reservoirs

Giles Exley¹, Trevor Page¹, Freya Olsson^{1,2}, Stephen J. Thackeray³, Michael J. Chipps⁴, Alona Armstrong^{1,5} and Andrew M. Folkard^{1,*}

Received: 30 September 2024 / Accepted: 12 September 2025

Abstract – Deployment of floating photovoltaics (FPVs) on water reservoirs is accelerating, and their lifetimes are expected to extend far into the 21st century. One of their potential co-benefits is mitigation of climate change-induced impacts on water quality. However, there has been little investigation of this possibility. We used MyLake, a 1D (vertical) numerical model, to simulate water quality impacts in a UK reservoir of different FPV coverages under four future climate scenarios and a present-day baseline case. We tested hypotheses that increased FPV coverage would offset climate-induced reservoir warming, stratification duration lengthening, phytoplankton biomass increases and taxonomic dominance changes. FPV coverage's ability to offset climate warming varied between the four climate scenarios, and seasonally within them. It was able to fully offset changes in stratification duration and to entirely prevent thermal stratification in all four future scenarios. Climate-induced increases in phytoplankton biomass and taxonomic dominance patterns were also entirely offset if sufficient FPV coverage was applied in all future scenarios. According to these results, FPV coverage will be able to compensate partially or fully for thermal and phytoplanktic changes in reservoirs under future climates. However, the amount of coverage required varies seasonally and depends on future climate trajectories.

Keywords: energy-environment interactions / phytoplankton / water quality / water temperature / FPV

1 Introduction

The present and future impacts of climate change on the water quality and quantity of reservoirs is a major concern for water supply companies and authorities. Observed and potential impacts of climate warming on lentic freshwater systems have attracted particular attention (e.g., Woolway et al., 2020; Rose et al., 2023). These impacts are highly socioeconomically significant in reservoirs, given that they are essential for providing drinking water and other ecosystem services. Climate warming has been linked to increases in mean water temperature (O'Reilly et al., 2015) and the duration of thermal stratification (Woolway and Merchant, 2019). These effects propagate throughout reservoirs bringing about, for instance, reduced oxygen concentrations (Jane et al., 2021), increased phytoplankton biomass (Winder and Sommer, 2012) and switches in taxonomic composition, which can favour toxin-producing species (Paerl and Huisman, 2009).

At the same time, there is rapid growth in the installation on reservoirs of floating photovoltaic solar panels (FPVs) for electricity generation (Nobre *et al.*, 2024). They are being deployed most commonly on raw water reservoirs, which store water prior to treatment (Exley *et al.*, 2021b). FPV installations reduce land use conflicts, sparing land for agriculture, industry, and conservation. They offer enhanced generation efficiencies over roof-top and ground- mounted solar panels, because of the cooling effect of the host water body (Oliveira-Pinto and Stokkermans, 2020). In water scarce contexts, they offer the co-benefit of evaporation reduction alongside electricity generation (Jin *et al.*, 2023). In some cases, they have been deployed alongside hydroelectric generation installations, to optimise the use of existing transmission infrastructure and improve the power output profile (*e.g.*, Silverio *et al.*, 2018).

FPVs have an expected 20- to 30-year lifespan, representing a long-term perturbation to the hosting water body (Costa and Silva, 2021). Since their first commercial deployment in 2007, knowledge of FPV-environment interactions has been gradually expanding. However, existing

¹ Lancaster Environment Centre, Lancaster University, Lancaster, LA1 4YQ, UK

² Department of Biological Sciences, Virginia Tech, Blacksburg, Virginia, USA

³ UK Centre for Ecology & Hydrology, Library Avenue, Bailrigg, Lancaster, LA1 4AP, UK

⁴ Thames Water Research, Development and Innovation, Kempton Park AWTW, Feltham Hill Road, Hanworth, TW13 6XH, UK

⁵ Energy Lancaster, Lancaster University, Lancaster, LA1 4FY, UK

^{*}Corresponding author: a.folkard@lancaster.ac.uk

predictions of FPV impacts are based only on present climate conditions (e.g., Exley et al., 2021b). The effects of FPVs on key water quality parameters under present conditions have been found to generally counteract those of climate change, offering the potential for FPV deployment to be used as a climate change mitigation tool. For example, FPV installations can reduce water temperatures (Liu et al., 2023), and shorten stratification duration (Ilgen et al., 2023), with the magnitude of the effect modulated by FPV coverage and deployment location (Exley et al., 2021a). These changes, along with impacts on the underwater light climate (Bax et al., 2023), have consequences for the biological functioning of the host water body, reducing phytoplankton growth and altering species composition; potential co-benefits that could improve water quality. However, the nature and scale of these effects is unknown under future climates. Different FPV coverage may be required to achieve the effects found under present climates. If FPVs can offset future climate impacts on reservoirs, they could delay or obviate the need for the costs of alternative interventions, such as new infrastructure for treating high concentrations of toxic phytoplankton species.

Decisions regarding installations of FPV are currently made in a context of widespread concern about the combined impacts of climate warming and other anthropogenic stressors on water quality and quantity in reservoirs (Benjamins et al., 2024). It is therefore essential to understand energyenvironment interactions associated with FPV to optimise their deployment, minimise detrimental effects and maximise benefits under both present and future climates (Armstrong et al., 2020). To address this need, we explored the combined effects of climate warming and FPV installation upon four of the likely effects of climate warming for reservoirs: increased water temperature, longer duration of thermal stratification, greater phytoplankton biomass, and changes in phytoplankton taxonomic composition that favour toxin-producing species. To achieve this, we used a numerical model to simulate the effects of FPV deployments on a raw water reservoir under plausible future climate scenarios. Furthermore, we explored how these effects are likely to vary with the percentage coverage of FPV on the water body surface and the severity and timescale of the climate changes. Specifically, we tested the hypotheses that increased FPV coverage under future climate scenarios would:

- 1. offset reservoir warming;
- 2. reduce the duration of thermal stratification; and
- 3. limit the growth of phytoplankton and alter their taxonomic composition.

We use insights gained from testing these hypotheses to assess potential implications for reservoir management of increased use of FPV deployment in the context of warming climates through the 21st century.

2 Materials and methods

We extended the methodology of Exley *et al.* (2022). A summary of the original methods and full details of the additional methods used to simulate future climate impacts are described below.

2.1 Site description

We modelled the effects of FPV coverage and climate changes on the Queen Elizabeth II reservoir (QEII, Fig. 1), a raw water reservoir located in south-west London, UK (51° 23' 27'' N, $0^{\circ} 23' 32'' \text{ W}$). The QEII has a surface area of 1.28 km², a mean depth of 15.3 m, a maximum depth of 17.8 m, and a volumetric capacity of 19.5 gigalitres $(1.95 \times 10^7 \,\mathrm{m}^3)$. It is steep-sided and approximately flat bottomed. Water is fed into the reservoir from the adjacent River Thames, pumped in through three inlets in its bed and abstracted at a single outlet tower at its north-eastern corner. Given the circulation patterns observed in the reservoir (Ta, 2019), it can be apportioned into two hydrographic zones: one relatively short residence time, faster-flowing zone (70% of surface area), in which the water moves relatively rapidly from the inlets to the outlet, and one comparatively longer residence time, slower-flowing zone (30% of surface area), which is largely circumvented by the faster flowing water. A FPV installation was installed on the slower-flowing zone of the reservoir in 2016, covering approximately 4.5% of the total reservoir surface.

2.2 MyLake model description

To carry out the modelling, we used MyLake v2 (Markelov et al., 2019), an expanded version of the well-established, open source, one-dimensional (vertical) numerical lake model MyLake (Saloranta and Andersen, 2007). MyLake v2 uses a daily time step to simulate 1 m vertical distributions of water temperature, phytoplankton, and dissolved and particulate substances, as well as interactions at the sediment-water interface.

Specifically, we used the version of MyLake v2 adapted by Exley et al. (2022) to enable simulation of differently functioning but connected 'zones' within a single water body, and to enhance phytoplankton representation by discriminating broad functional groups. This was tested against empirical data by Exley et al. (2022) and found to perform well. Because the focus of the study reported here is future forecasts, it cannot be tested against empirical data specific to its outputs. Although MyLake is a one (vertical) dimension model, to provide a basic representation the hydrodynamics of the QEII reservoir, the model was set up to comprise a shorter residence time, fasterflowing zone and a longer residence time, slower-flowing zone. Although, in the reservoir, these have a specific spatial configuration defined by bathymetry and the location of the inlets and outlet, in the model they were represented by 1Dvertical domains - essentially two MyLake models running side by side. These two models were linked via an eddy diffusion matrix, which governed the amount of lateral mixing between them, and an advection matrix, which specified the flows between them. Both the diffusion and advection matrices were set to exchange 2.5% of volume between the models during each simulation time step. This is based on the one day - of the order of 10^5 s - time step and the size of the smaller (slower-flowing) zone of the order of 500 m, assuming a diffusivity coefficient of the order of 10^{-2} m²s⁻¹, typical of lateral diffusion in slow flowing water (e.g., Schnoor, 1996) and that advective and diffusive transport are of the same order of magnitude in this setting.

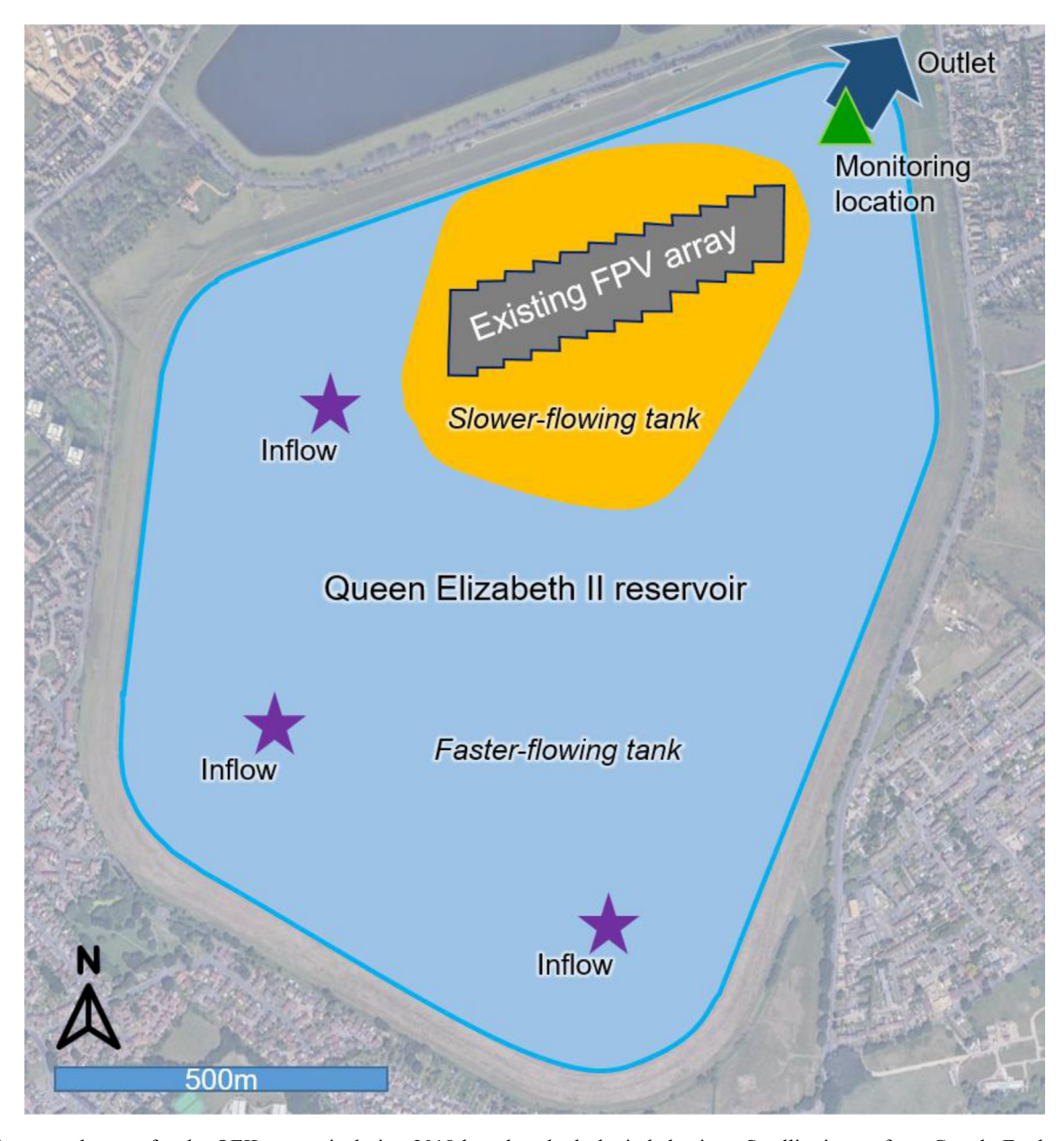


Fig. 1. Conceptual zones for the QEII reservoir during 2018 based on hydrologic behaviour. Satellite image from Google Earth.

2.3 Future climate scenarios

To drive the model, we used a subset of the meteorological scenarios from the United Kingdom Climate Projections 2018 (UKCP18) daily global (60 km resolution) projections for the Thames basin (UK Meteorological Office Hadley Centre, 2018). These are based on multiple variants of the HadCM3 climate model (Lowe *et al.*, 2019). Two Representative Concentration Pathways (RCPs) were used: RCP2.6 and RCP8.5. RCP2.6 represents a future with significant reductions to greenhouse gas emissions, where radiative forcing will increase by 2.6 Wm⁻² by 2100. RCP8.5 represents a scenario with unabated, very high greenhouse gas emissions, leading to an increase in radiative forcing of 8.5 Wm⁻² by 2100. These two scenarios envelope a range of plausible future climates (Lowe *et al.*, 2019).

We simulated four cases, defined by mid-century and late-century conditions for each of the RCP2.6 and RCP8.5 scenarios: RCP2.6_{2040–2069}, RCP8.5_{2040–2069}, RCP2.6_{2070–2099} and RCP8.5_{2070–2099}. Each case is simulated over one year, using driving data derived from the mean of each of these 30-year windows of UKCP18 projections, thereby removing interannual variability from our analyses. To compare between future and present conditions, we defined a fifth, baseline case using the mean of the RCP2.6 projections for the 30-year window 2003–2033.

The 30-year averaging process used to arrive at these scenarios smoothed out variability at daily timescales. To add such variability back in, meteorological data from 2018 were used. To define the daily variability signature, raw observations of global radiation, cloud cover, wind speed, air temperature and relative humidity from the closest meteorological station

Table 1. Parameterizations of phytoplankton functional groups used in the model (from Exley et al., 2022).

| Parameter | | Range sampled (min., max. or fixed) | | | | | |
|----------------------------------------------------------------------------------|-------|-------------------------------------|-----------|---------|-----------|---------------|-----------|
| | | Diatoms | | Greens | | Cyanobacteria | |
| PAR saturation level for growth (mol-quanta m ⁻² s ⁻¹) | | 0.000025 | | 0.0005 | | 0.00075 | |
| | | 0.000045 | | 0.00075 | | 0.0009 | |
| Optical cross section of chlorophyll-a (m ⁻² mg ⁻¹) | Fixed | 0.03 | | 0.005 | | 0.01 | |
| Loss rateat 20 °C (day ⁻¹) | | Grazed | Un-grazed | Grazed | Un-grazed | Grazed | Un-grazed |
| | Fixed | 0.18 | 0.13 | 0.05 | 0.025 | 0.025 | 0.0125 |
| Settling velocity (m day ⁻¹) | Fixed | | 0.3 | 0.05 | | 0.005 | |
| Specific growth rateat 20 °C (day ⁻¹) | Min | in 0.7 | | 1 | | 1.1 | |
| | Max | 1.1 | | 2 | | 1.8 | |
| Half saturation growth P level (mg m ⁻³) | Fixed | | 5 | | 5 | | 5 |
| Half saturation growth N level (mg m ⁻³) | | Grazed | Un-grazed | Grazed | Un-grazed | Grazed | Un-grazed |
| | Fixed | 80 | 80 | 80 | 80 | 80 | 0.1 |
| Half saturation growth Si level (m gm ⁻³) | Fixed | | 550 | | - | | _ |
| If algae are N-Limited | | Grazed | Un-grazed | Grazed | Un-grazed | Grazed | Un-grazed |
| | Fixed | 1 | 1 | 1 | 1 | 1 | 1 |
| If algae are Si-Limited | Fixed | | 1 | | 0 | | 0 |
| Scaling factor for inflow concentration of chlorophyll- <i>a</i> (dimensionless) | Fixed | | 0.5 | | 0.4 | | 0.1 |

(London Heathrow, 10 km away) for the whole of 2018 were smoothed using a five-day moving average and the daily difference between the moving average and the raw observation calculated. These differences between the five-day average and the daily values were added back into the 30-year averaged data on the corresponding day of the year. For example, if the air temperature on, say, the 20th March 2018 was 0.5 °C above the average air temperature of the five days centred on that date (*i.e.*, 18^{th} – 22^{nd} March), then 0.5 °C was added to the air temperature value in each of the four 30-year averaged data sets used in the simulations. Daily air pressure and rainfall recorded at Heathrow Airport (UK Meteorological Office, 2019) were kept the same for all five modelled scenarios.

2.3.1 Inflow temperature and volume

A data-based transfer function (TF) model was used for estimating inflow water temperature from air temperature and global radiation under present and future climates. The model is a discrete-time TF derived directly from the available data (Environment Agency, 2018; UK Meteorological Office, 2019; Findlay, 2022) using the Refined Instrumental Variable (RIV) algorithm (Young, 2015) implemented within the CAPTAIN Toolbox for MatlabTM (Taylor *et al.*, 2007). The resulting model structure has the multi-input single-output model

$$\begin{split} T_{R_t} &= 1.794 T_{R_{t-1}} + 0.794 T_{R_{t-2}} + 0.1609 T_{a_{t-1}} \\ &+ 0.0278 R_{g_{t-1}} - 0.1604 T_{a_{t-2}} - 0.0278 R_{g_{t-2}} \end{split} \tag{1}$$

where T_R is river temperature, T_a is air temperature, R_g is global radiation and the subscripts t, t-1, t-2 indicate the current and antecedent time steps, respectively. Future inflow volumes were predicted from projected river flows at Kingston-upon-Thames (\sim 8 km downstream of Q EII) (Prudhomme *et al.*, 2013). The use of river flows as a proxy for changes in water available for abstraction from the river assumes no changes to management or water demand. Mean

daily river flow for each day of the year was computed for a 30-year window centred on 2018 (2003–2033), and the difference compared to river flow in 2040–2069 and 2070–2099. A moving average was applied to calculate the change in daily river flow as a percentage of present-day flow. For the mid-century and late-century cases, percentage changes in reservoir inflow volume were assumed to equal the percentage change in river flow, thus inflows that varied daily were synthesized. In the baseline case, we assumed no change to reservoir inflow volumes. Reservoir volume was maintained constant for all cases.

2.3.2 Phytoplankton data

Six functional groups of phytoplankton were simulated to reflect broadly the species composition observed in the QEII reservoir at the reservoir outlet during 2018: these comprised grazed and ungrazed groups of each of diatoms, green algae and cyanobacteria. Grazing pressures (represented by loss rate), size, growth rate, light requirement for growth, and settling velocity varied among these groups. Here, we combine the grazed and ungrazed groups, thus reporting results for three groups: diatoms, green algae, and cyanobacteria. Full details on parametrisation of each functional group are as in Exley et al. (2022) and shown in Table 1.

2.3.3 Other model driving data

Two monitoring stations on the River Thames, located 5.5 km upstream (Wey tributary) and 11.6 km downstream (Teddington Weir) of the QEII inlet, were used to estimate inflow nutrient concentrations (Environment Agency, 2018). Samples (approximately monthly) were linearly interpolated to obtain mean daily values for 2018. The 2018 inflow nutrient concentrations were used for all cases. The resources available for phytoplankton growth did not change in our simulated scenarios, allowing us to discern the effects of climate change

Table 2. Percentage coverage of each of the two zones into which the model divided the reservoir, for each of the incremental total FPV coverage model runs. All values are shown as a % of the total reservoir surface area.

| Total FPV surface coverage | Faster flow zone covered | Faster flow zone uncovered | Slower flow zone covered | Slower flow zone uncovered |
|----------------------------|--------------------------|----------------------------|--------------------------|----------------------------|
| 10 | 10 | 60 | 0 | 30 |
| 20 | 20 | 50 | 0 | 30 |
| 30 | 30 | 40 | 0 | 30 |
| 40 | 40 | 30 | 0 | 30 |
| 50 | 45 | 25 | 5 | 25 |
| 60 | 50 | 20 | 10 | 20 |
| 70 | 55 | 15 | 15 | 15 |
| 80 | 60 | 10 | 20 | 10 |
| 90 | 65 | 5 | 25 | 5 |
| 100 | 70 | 0 | 30 | 0 |

on reservoir properties without any confounding effects of resource variability. Bathymetry for QEII was digitised from a 2004 1m-resolution survey provided by the reservoir operator.

2.4 FPV deployments under future climate simulations

We varied FPV surface coverage between model runs in 10% increments from 0–100%. As the two zones into which the model divides the reservoir are unequal in surface area, initially, the array was placed entirely on the larger of the two zones (the faster flow zone). As the percentage surface coverage increased, when the faster flowing zone's remaining exposed area equalled that of the slower flowing zone, the array was deployed equally between the two zones. Table 2 provides a detailed breakdown of zone coverages for each overall coverage.

We assumed that under the FPV coverage global radiation was decreased by 94% and wind speed was lowered by 95%. These assumptions are based on observations made at an FPV installation near Lancaster, UK (Exley *et al.*, 2022) and a landbased solar park near Swindon, UK, (Armstrong *et al.*, 2016).

2.5 Model calibration

MyLake had already been calibrated for use on the QEII reservoir (Exley et al., 2022), using the Generalised Likelihood Uncertainty Estimation (GLUE) procedure (Beven and Binley, 1992). We used formalised limits of acceptability to account for the uncertainty associated with modelling environmental systems, following Exley et al. (2022) and based on the method and expert based estimates first described by Page Page T, et al. (2017). We compared model output from multiple simulations with observed data (total chlorophyll-a, surface water temperature, stratification duration and phytoplankton functional group proportions) to identify acceptable baseline simulation results and parameter sets. Acceptable simulations are defined by a fuzzy weighting function that returns a relative confidence for each simulation depending on its position within the formalised limits of acceptability. To limit bias within the parameter sets, the parameter ranges comprised physically reasonable values for each parameter and were

sampled 8,000 times using a Monte Carlo strategy. Seventy-five parameter sets were within the limits of acceptability for all simulations; the remaining 7,925 parameter sets were rejected and not used in the subsequent analyses.

2.6 Model output analysis

To summarise the impact of varying FPV coverage under different predicted future climates, we compared model output from each of the four future cases with that from the baseline case, for each of the coverage scenarios (Tab. 2). Our analysis focused exclusively on the faster-flowing zone, as this contains the reservoir outflow and therefore determines the quality of water entering the treatment works. We analysed water temperature at 1 m depth and the stratification duration. We used two metrics to define the latter. These were maximum stratification (the longest period of continuous stratification) and cumulative stratification duration (the total number of stratified days during the one-year simulation period). Stratification was defined using a threshold density gradient of $0.1\,\mathrm{kg}\,\mathrm{m}^{-3}~\mathrm{m}^{-1}$ between adjacent 1 m layers. For phytoplankton composition, each functional group was represented as a proportion of the total biomass (using chlorophyll-a as a proxy) at 1 m depth.

The variability amongst the 75 model outcomes produced for each climate scenario was captured used the median, $2.5^{\rm th}$ and $97.5^{\rm th}$ percentiles of the values obtained for each variable (yielding the associated 95% confidence interval). We present the maximum ($T_{\rm max}$) and minimum ($T_{\rm min}$) water temperature, maximum and cumulative stratification duration, and maximum total chlorophyll-a concentration (Chl- $a_{\rm max}$) for each season, defined as: winter — December to February; spring — March to May; summer — June to August; autumn — September to November. Phytoplankton species composition is presented as a time series for the simulated year. Given the volume of data, some FPV coverage extents are omitted from the figures here.

3 Results

3.1 The effect of FPV coverage on water temperature

In all the future cases, $T_{\rm max}$ was raised relative to the baseline case in every season, with warming increasing

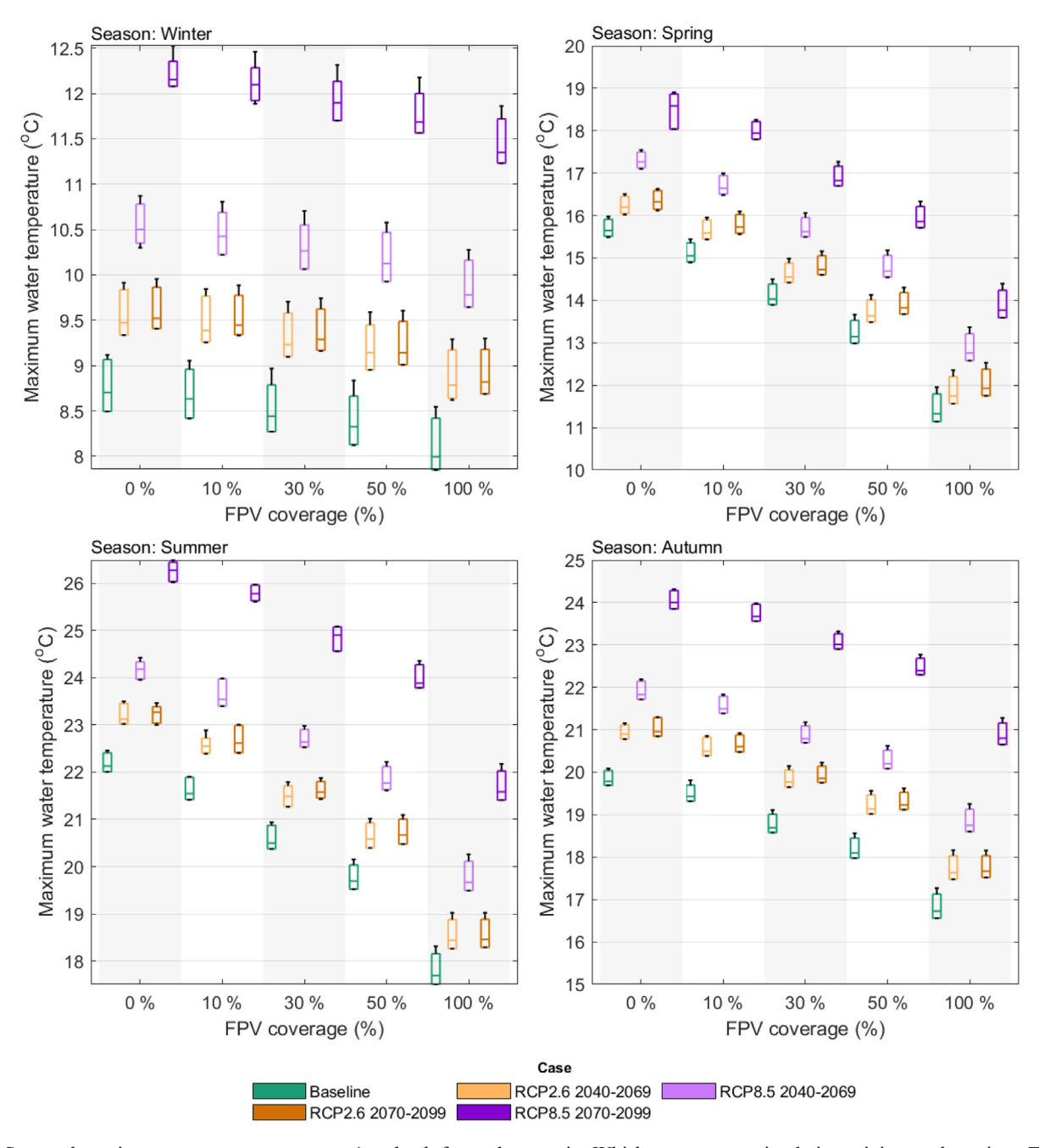


Fig. 2. Seasonal maximum water temperatures at 1 m depth for each scenario. Whiskers represent simulation minima and maxima. The box represents the 2.5th & 97.5th percentiles. 0% FPV coverage represents QEII reservoir simulated as a baseline case with no additional FPV coverage.

between the mid-century and late-century cases for each RCP (Fig. 2). Increasing FPV percentage coverage progressively cooled $T_{\rm max}$ in all seasons. FPV coverage was able to fully offset changes to $T_{\rm max}$ in spring and summer for all four future cases, although the amount of coverage required to do this increased from RCP2.6 to RCP8.5, and from mid-century to late-century. In spring, the increases of $T_{\rm max}$ in the RCP2.6 cases was offset by FPV coverages of 10% in mid-century and 20% in late century. For the RCP8.5 cases, these "offset coverages" were 30% and 60%, respectively. In summer, greater offset coverages were required. For the two RCP2.6 cases, they were 20% (mid-century) and 30% (late century),

and for the RCP8.5 cases, they were 40% and 90%, respectively. In autumn, changes to $T_{\rm max}$ were offset by FPV coverages of 30% (mid-century) and 40% (late-century) for the RCP2.6 cases and 70% for the RCP8.5 mid-century case. In the RCP8.5 late-century case, even 100% FPV coverage was unable to fully offset the increase in $T_{\rm max}$. During winter, no extent of FPV coverage was able to offset fully the changes to $T_{\rm max}$ in any of the future cases.

As for $T_{\rm max}$, and in line with our hypotheses, $T_{\rm min}$ increased in the future cases compared to the present day, and from mid-century to late-century (Fig. 3). Increasing FPV coverage cooled $T_{\rm min}$ in all cases. It was less effective at

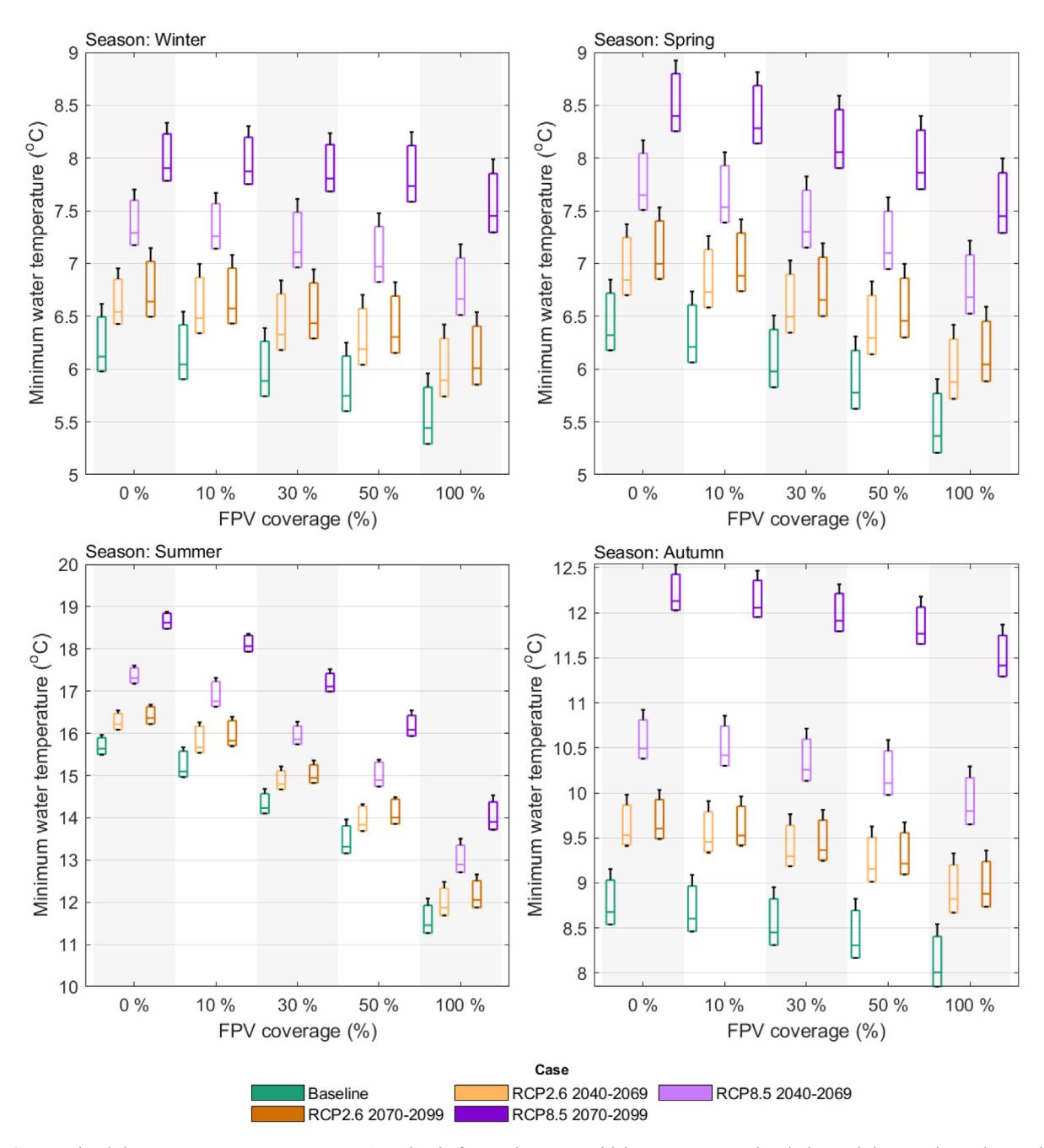


Fig. 3. Seasonal minimum water temperatures at 1 m depth for each case. Whiskers represent simulation minima and maxima. The box represents the 2.5th & 97.5th percentiles. 0% FPV coverage represents QEII reservoir simulated as a baseline case with no additional FPV coverage.

offsetting climate warming effects on $T_{\rm min}$ than $T_{\rm max}$. Even 100% FPV coverage was unable to offset $T_{\rm min}$ increases in winter, spring, or autumn in both RCP8.5 cases, or in autumn for both RCP2.6 cases. FPV coverages of 70% and 90% were required to offset winter $T_{\rm min}$ warming in the RCP2.6 mid-century and late-century cases, respectively. In spring, FPV coverages of 50% and 70% offset climate warming of $T_{\rm min}$ for the RCP2.6 mid-century and late-century cases, respectively. Summer $T_{\rm min}$ increases were offset by 20% FPV coverage in both RCP2.6 cases and by 40% and 70% FPV coverage for the RCP8.5 mid-century and late-century cases, respectively.

3.2 The effect of FPV coverage on stratification duration

Compared to the simulated effects upon water temperature, there was relatively high among-simulation variability in stratification duration for each climate change case, compared to the differences among cases. With no FPV coverage, average maximum stratification duration remained the same as in the baseline case for the two mid-century cases, reduced by four days for the RCP2.6 late-century case, and increased by two days for the RCP8.5 late-century case (Fig. 4). FPV coverage of 10% reduced maximum stratification duration by

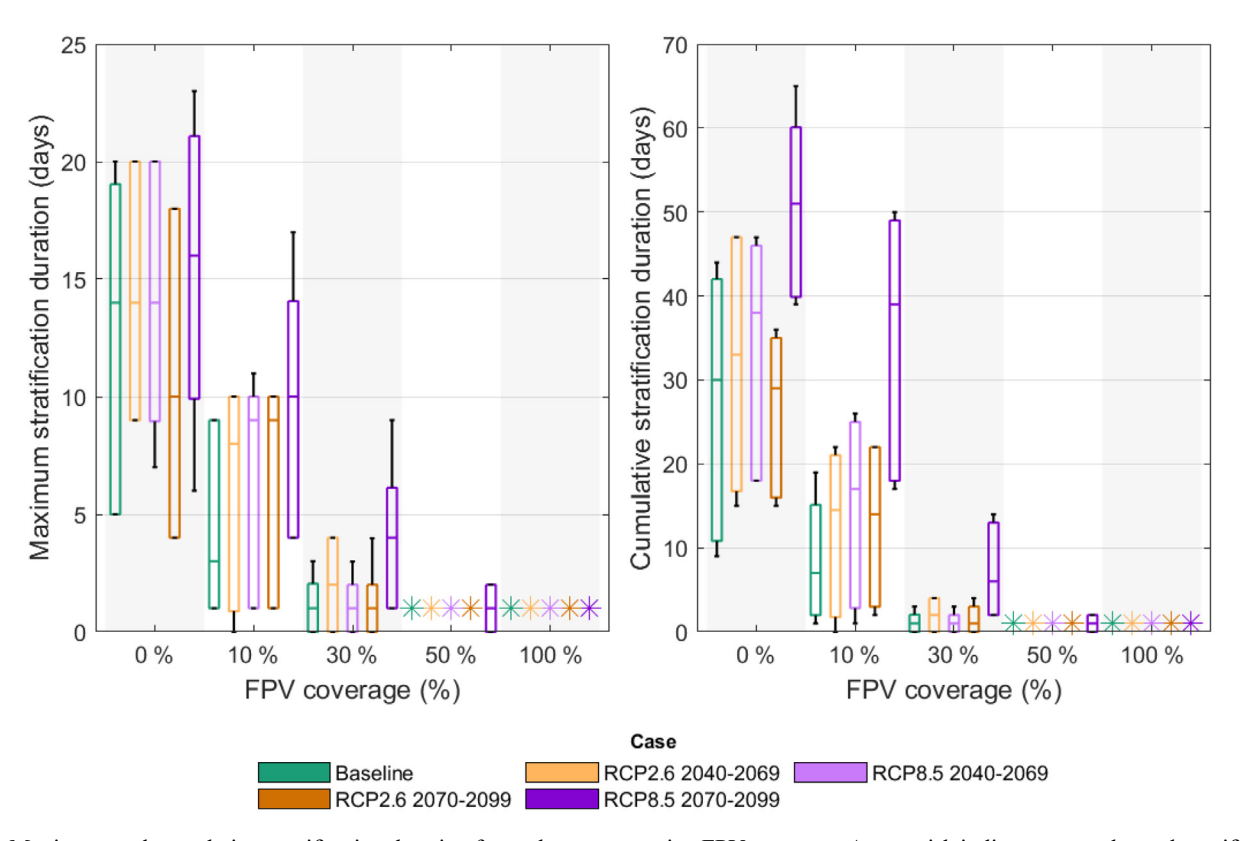


Fig. 4. Maximum and cumulative stratification duration for each case at varying FPV coverage. An asterisk indicates no prolonged stratification event occurred for the simulation. Whiskers represent simulation minima and maxima. The box represents the 2.5th & 97.5th percentiles. 0% FPV coverage represents QEII reservoir simulated as a baseline case with no additional FPV coverage.

eleven days for the baseline case and caused smaller reductions in the future cases: six and five days by mid-century for the RCP2.6 and RCP8.5 cases, respectively, and five and four days for the corresponding late-century cases.

Cumulative stratification duration increased by three days for the RCP2.6 mid-century case, eight days for the RCP8.5 mid-century case and 21 days for the RCP8.5 late-century case but reduced by one day for RCP2.6 late-century case compared to the baseline case. The increase in cumulative stratification from climate change was offset by 10% FPV coverage for the mid-century cases and 20% coverage for the RCP8.5 late century case. The reservoir experienced no stratification when FPV coverage exceeded 40% for both RCP2.6 cases and the RCP8.5 mid-century case. For the RCP8.5 late-century case, a 60% or greater FPV coverage prevented any thermal stratification.

3.3 The effect of FPV coverage on phytoplankton biomass and species composition

With no FPV cover, Chl- $a_{\rm max}$ increased in all the future cases in comparison to the baseline case (Fig. 5). The largest increases occurred in the summer under the late-century RCP8.5 case (>25 μ g L⁻¹). Increases to spring, summer and autumn Chl- $a_{\rm max}$ compared to the baseline case were offset at 10% FPV coverage for both RCP2.6 cases and the RCP8.5 mid-century case. A greater FPV coverage of 20% was required to offset increases in spring, summer and autumn Chl- $a_{\rm max}$ for the RCP8.5

late-century case. FPV coverage above these thresholds led to substantial reductions in Chl- $a_{\rm max}$ for all future climate cases compared to the baseline case with 0% FPV coverage.

Whilst simulated Chl- $a_{\rm max}$ concentrations declined rapidly with increasing coverage (Fig. 5), the relative proportions of phytoplankton functional groups varied (Fig. 6). In the baseline case without FPV coverage, diatoms are the most dominant functional group throughout the year, except for August to September, when green algae and cyanobacteria concentrations peak and the former exceeds the diatom concentration briefly. In the baseline climate scenarios in general, FPV coverage reduces the peaks in green algae and cyanobacteria and enhances the dominance of diatoms. The exception is the 100% coverage case, in which green algae concentration is higher than in the baseline case throughout the year and matches that of the diatoms in late summer and early autumn.

Under the future climate cases, the 0% FPV coverage results show increased peaking of the green algae and cyanobacteria and enhanced declines in diatoms in the later summer and early autumn. This results in green algae becoming the dominant functional group at this time in all cases, with cyanobacteria also exceeding diatoms in both RCP8.5 cases. As FPV coverage increases, however, this effect is reduced, and the results for all future climate cases move closer to the baseline case results. For all coverages of 30% and above, the results of the baseline case and all future climate cases are essentially indistinguishable. Note also that, given the reductions in total chlorophyll-a

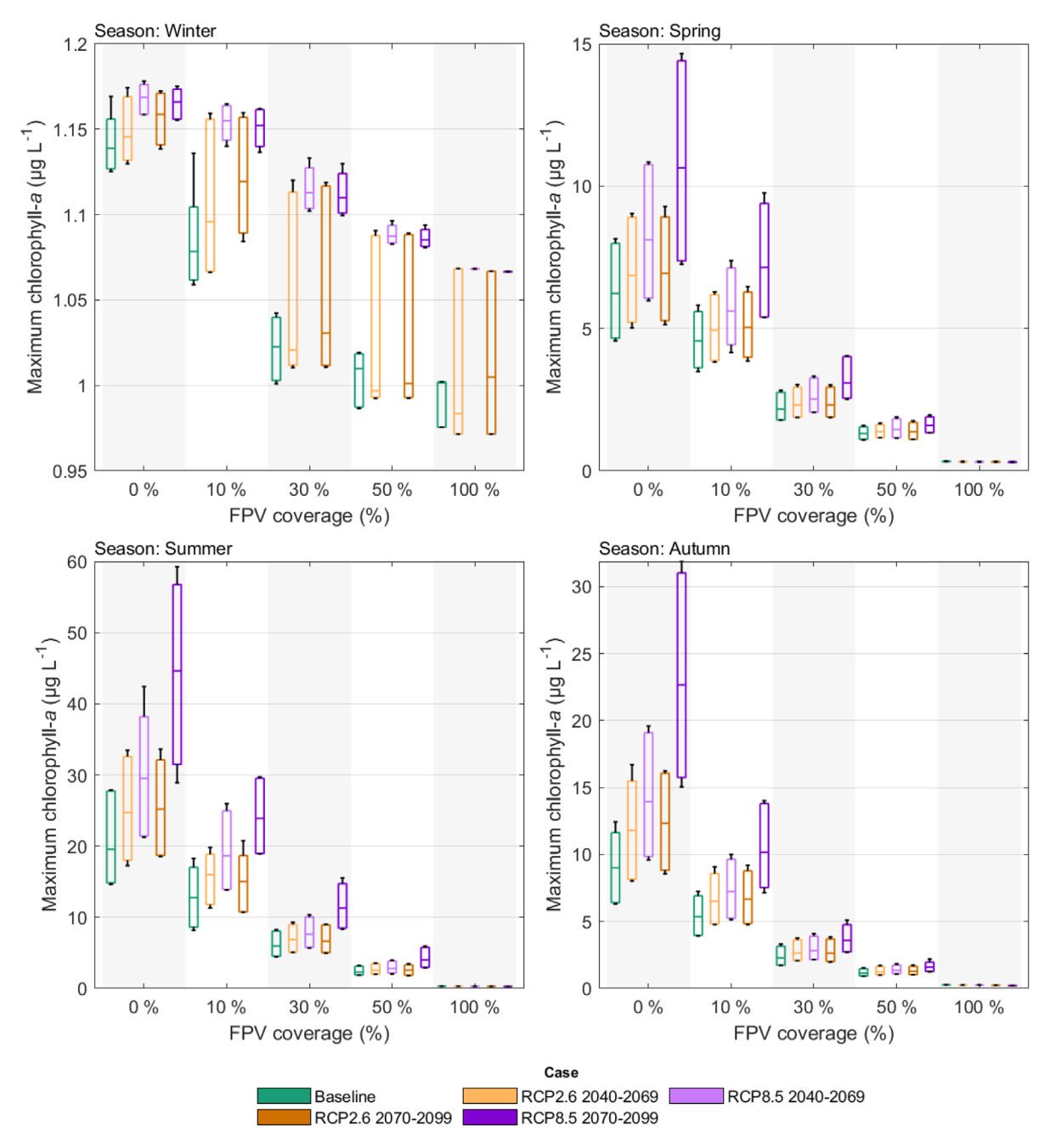


Fig. 5. Seasonal maximum chlorophyll-a at 1 m for each case with varying FPV coverage. Whiskers represent simulation minima and maxima. The box represents the 2.5th & 97.5th percentiles. 0% FPV coverage represents QEII reservoir simulated as a baseline case with no additional FPV coverage.

with increasing FPV cover (Fig. 5), these functional group percentages are of a lower overall concentration.

4 Discussion

The results presented show the potential for FPV to offset some future climate change impacts in reservoirs, although the extent to which that could be achieved varies with season, climate scenarios and time horizons, percentage cover and waterbody properties.

4.1 The ability of FPV coverage to offset water temperature warming

Mitigation of the impacts of ongoing long-term climate change-induced warming of reservoirs and more frequent heatwaves are an important potential co-benefit of FPV deployment. Changes in reservoir heat budgets are predicted to alter the structure and functioning of freshwater ecosystems, which will, in turn, undermine the provision of key services and benefits to people including clean water provision, fisheries, tourism, and recreation (Saulnier-Talbot and Lavoie,

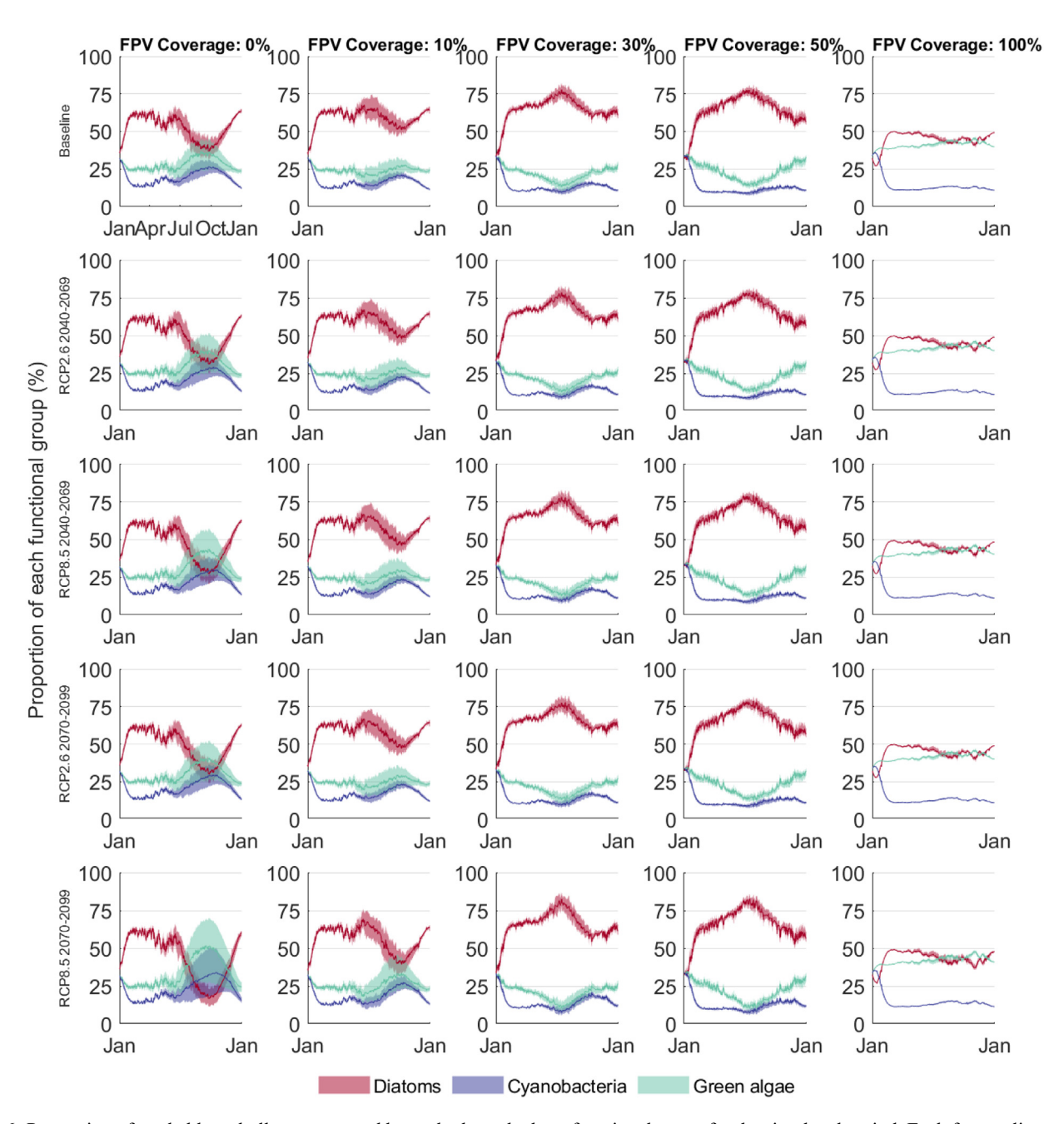


Fig. 6. Proportion of total chlorophyll-a represented by each phytoplankton functional group for the simulated period. Each future climate case and a subset of the simulated FPV coverage is shown. The initial phytoplankton functional group proportions were set evenly, therefore, the first 30 days of simulations are model run-in time. 0% floating solar coverage represents QEII reservoir simulated as a baseline case.

2018). Long-term reservoir warming may lead to phenological change (Thackeray et al., 2016) and food-web de-synchronisation (Thackeray et al., 2013), while periods of extreme heat could lead to fish die-offs when temperatures exceed species' thermal tolerances (Miranda et al., 2020). Such events can degrade water quality, affect reservoir operations, and raise public concerns about decomposition odours (Godinho et al., 2019). Climate warming could also accelerate organism metabolic rates, with far-reaching ecological implications. These include potential effects on greenhouse gas emissions; accelerated reservoir metabolism can increase methane and

carbon dioxide emissions, contributing to further climate warming (Kraemer et al., 2017).

According to our results, increasing FPV deployment decreases the maximum water temperature in all the scenarios considered, in agreement with *in situ* measurements reported by, for example, Ilgen *et al.* (2023). This raises the question of whether it may offer an effective means to mitigate against climate-induced warming of reservoirs. In terms of our first hypothesis, FPV coverage was able to fully offset increases to maximum seasonal temperatures in the spring and summer in our model but was only able to do so in autumn for the lower

emissions RCPs and was only able to partially offset climatic warming in winter. FPV was less effective at offsetting increases to minimum seasonal temperatures, especially during winter, spring, and autumn. However, it still provided a dampening effect, limiting water temperature increase under climate change.

In seasons where FPV coverage was unable to fully offset the QEII reservoir's future warming, a likely cause is the relative temperature of the inflow and outflow. In the cooler months of the year, inflows to reservoirs tend to be warmer than their outflows, leading to net heating (Livingstone and Imboden, 1989) that cannot be counteracted by the seasonally-diminished shading and sheltering effects of FPVs. Given the short residence time of the reservoir, this heat flux is likely to be an important element of the reservoir's heat budget (Fenocchi et al., 2017). However, these inferences about future scenarios from the perspective of physical science need to be considered together with potential changes in reservoir management and water demand to gain a better predictive capability regarding water temperature.

Reductions in future minimum water temperatures caused by FPV coverage in winter (Fig. 3) may be considered problematic by reservoir operators who are responsible for public water supplies. Reduced water temperatures (to below 5 °C), as seen with increasing FPV coverage in the baseline case, could lead to increased risk of the water distribution network suffering from pipe contraction, increasing the incidence of bursts (Jesson *et al.*, 2010) and consequent problems for water supply and potentially damaging surrounding infrastructure (Mora-Rodríguez *et al.*, 2015).

4.2 The ability of FPV coverage to offset stratification duration increases

Our simulations supported our second hypothesis that FPV coverage can reduce stratification duration. Again, this is in agreement with the in situ measurements reported by Ilgen et al. (2023). Thermal stratification is one of a reservoir's most important physical characteristics, and prolonged stratified periods can degrade water quality by changing biological and chemical processes (Woolway et al., 2021). Periods of thermal stratification can facilitate oxygen depletion in bottom waters (where oxygen is used for biological and chemical processes) by preventing oxygen replenishment from the surface (Boehrer and Schultze, 2008). Oxygen depletion can have wide-ranging impacts on reservoir function, often acting as a catalyst for water quality problems. For example, hypoxia could lead to fish die-off events in productive reservoirs, degrading water quality and disrupting food webs (Till et al., 2019). Further, deoxygenation of bottom waters due to prolonged stratification duration may facilitate the internal loading of phosphorus from bed sediments, fuelling phytoplankton blooms that reduce water quality and reservoir amenity (North et al., 2014). Stratification-induced anoxia may also increase methane production from reservoirs (Vachon et al., 2019). However, FPV coverage may limit surface exchanges of dissolved oxygen, given reduced wind shear at the air-water interface (Andini et al., 2021). Therefore, reservoir oxygen levels could still be lower than in the baseline case, particularly at greater FPV coverage, even with reduced stratification duration

(Chateau *et al.*, 2019). Destratification strategies currently used in the water industry include pumped water circulation or introducing air curtains and add to annual reservoir management costs. Electrical power is required for this purpose, so the reduction in stratification, combined with the potential use of renewable energy from the FPV may be attractive. This is an issue that requires further exploration.

Under future climates there was an increase in maximum stratification duration (for the RCP8.5 mid-century case) and increased cumulative stratification duration (for the RCP2.6 mid-century and both RCP8.5 cases), suggesting a potential threat to water quality. However, only modest FPV coverage was required to achieve substantial reductions in stratification duration. For example, in the RCP8.5 late-century case, an FPV coverage of 30% reduced the median cumulative stratification duration by 88%. Such changes could have significant benefits for water body processes, properties, and ultimately ecosystem service delivery.

Whilst FPV coverage successfully reduced stratification duration, offsetting the effects of future climates, stratification events in QEII were often short regardless. The increases to cumulative stratification duration in OEII under future climate conditions demonstrate a discontinuous polymictic mixing regime, characterised by short irregular stratified periods that are disrupted by frequent mixing events. Even under the higher climate warming scenario (RCP8.5 latecentury case), the maximum stratified period lasted for a median of 16 days, a period brief enough for complete anoxia to be unlikely, although, partial deoxygenation may occur in sufficiently productive reservoirs (Jane et al., 2021). However, in years with low wind speeds, low inflow or higher air temperatures, the mixing regime could shift to monomictic, characterised by a single period of prolonged stratification, increasing the likelihood of detrimental deoxygenation events. In other water bodies that exhibit prolonged stratification, the ability of FPV coverage to limit increases to stratification duration under future climates may improve reservoir water quality.

4.3 The ability of FPV coverage to limit the growth of phytoplankton and alter their taxonomic composition

Climate change-induced reservoir warming is likely to lead to an increased prevalence of cyanobacteria and more frequent blooms (Paerl and Huisman, 2009). Cyanobacterial blooms can cause oxygen depletion, increase turbidity and release toxins. Different water treatment processes may be required to mitigate these impacts, increasing water treatment costs (Watson *et al.*, 2016). Cyanobacterial blooms can also affect recreational ecosystem services, as they pose a health risk to humans, livestock, and pets.

In support of our third hypothesis, our simulations suggest that FPV coverage could limit the growth of phytoplankton and prevent dominance of cyanobacteria under future climates (Figs. 5 and 6). Increases in Chl- $a_{\rm max}$ concentrations under predicted future climates were offset with low FPV coverage (<20%) in all seasons. For example, in the late-century RCP8.5 case, summer Chl- $a_{\rm max}$ concentrations were simulated to increase by 128% in the QEII reservoir. However, 10% FPV coverage could limit this increase to just 22%, while a 30%

FPV coverage reduced summer Chl- $a_{\rm max}$ concentrations by 42% compared to the baseline case with no FPV coverage. However, future phytoplankton biomass and species composition will also be determined by inflow nutrient concentrations under future climates, which were not modified in this study.

Whilst FPV deployment may allow management of cyanobacterial growth, it could also trigger community turnover in favour of other taxa, such as diatoms. Filamentous diatoms and some colonial green algae can disrupt water treatment processes by blocking filters (Henderson *et al.*, 2008). Our model predicts that FPV coverage would reduce peaks in cyanobacteria and green algae between late summer and early autumn, allowing diatoms to proliferate. However, whilst FPV coverage of >10% increased the dominance of diatoms, the change was compensated by reductions in total chlorophyll-a concentration caused by FPV coverage.

4.4 The effectiveness of FPV as a tool for offsetting climate change impacts on reservoirs

FPV deployment presents dual benefits of providing lowcarbon electricity generation and potentially acting as a management tool for offsetting changes to water temperature, stratification duration, and phytoplankton growth under future climates. The FPV coverage required to achieve this offsetting varies by season. Our model predicts that mid-century summer maximum temperature changes would be offset with coverage of 20% (RCP2.6) or 40% (RCP8.5). The late-century cases have considerable variation in the FPV coverage required to offset changes in summer maximum temperature, given the large difference in emissions, with 30% (RCP2.6) and 90% (RCP8.5) required. The FPV coverage required to offset changes in summer Chl- a_{max} and cumulative stratification duration were considerably lower than for summer maximum temperature. Changes in summer $Chl-a_{max}$ and cumulative stratification duration were offset for both mid-century cases and for the late-century RCP2.6 case with 10% FPV coverage, with 20% FPV coverage sufficient to offset changes caused by the late-century RCP8.5 case.

However, our results should be interpreted with a degree of caution. Firstly, there are various limitations to the model itself, and therefore to the reliability of its predictions. Specifically, reduction of short wave solar radiation and wind energy are the only influences of FPV coverage that have been included in the model. For example, the impact on long wave radiation (in both directions), evaporation, and the impact of the arrays' wind and water wakes (which might be expected to have an influence on mixing and stratification beyond the physical footprint of the FPV) have been omitted. Further research is required to address the impact of these omissions. FPV coverage is not the only design feature of importance when making deployment decisions. Siting location on the host water body, for instance, can strongly mediate water body responses (Exley et al., 2022) and needs to consider aspects of reservoirs including surface water velocities, local water depth and the shading effects of fringing forestry or topography (Herlambang et al., 2024). Moreover, wider issues of technoeconomic viability (Alhassan et al., 2023) and social

acceptability and stakeholder collaboration (Benjamins et al., 2024) will guide FPV deployment roll out. We also acknowledge that our simulations focus exclusively on the OEII reservoir – and simplify and abstract its nature. It is likely that the potential ability of FPV coverage to offset climate change impacts will vary across climate zones. Finally, our simulations suggest that a very high FPV coverage would be required to fully-mitigate projected water temperature warming under the late-century high emissions (RCP8.5) case. However, such high FPV coverages may be incompatible with other water body uses, such as water sports, fishing or other recreational activities (Exley et al., 2021b). Further, high FPV coverage may have other impacts on the hosting water body not simulated in this study. For example, reduced sunlight under an FPV array limits the UV degradation of dissolved organic carbon (Armstrong et al., 2020) and pathogens (Mathijssen et al., 2020), an important form of natural water treatment. Much further research is required to understand potential unintended ecological impacts of FPV deployments and deliver operational guidance that can be followed with confidence.

4.5 Conclusion

The deployment of FPV on reservoirs is accelerating, and this growth is forecast to continue at a global scale as the energy transition continues. FPV deployment represents a long-term perturbation to a water body, so understanding its potential impacts under both present and future climates is vital to minimising unintended consequences. This study shows that reservoir managers can use FPV coverage to offset partially or fully, or even over-compensate for changes in reservoir water temperature, stratification duration, phytoplankton biomass and species composition under future climates. In this study, we have identified considerable differences in the FPV coverage required to achieve these offsets, depending on season, future emissions levels, and desired management goals. Higher FPV coverages are needed to offset water temperature changes in cases with higher emissions. However, lower FPV coverage were sufficient at offsetting changes to phytoplankton biomass at all emissions concentrations. FPV could be used as an effective tool for managing climate change impacts on reservoirs in addition to their primary role of providing electrical energy, but the specifics of each deployment must be considered to ensure suitability and preservation of water body ecosystem service provision.

Acknowledgements

GE was supported by a Natural Environment Research Council (NERC) Envision DTP Industrial CASE studentship (grant number NE/R010226/1) with United Utilities. AA was supported by a NERC Industrial Innovation Fellowship (grant number: NE/R013489/1). GE, TP and AA were also supported by the Lancaster University EPSRC IAA (grant number: EP/R511560/1) and a consortium of Affinity Water, South East Water, Southern Water and Thames Water. We are grateful to many colleagues at Thames Water for insights that have substantively improved this manuscript.

References

- Alhassan MO, et al. 2023. Techno-economic and environmental estimation assessment of floating solar PV power generation on Akosombo dam reservoir in Ghana. Energy Rep 10: 2740–2755.
- Andini S, et al. 2021. Evaluating the effect of floating photovoltaic on trophic state using mesocosm experiments, *Proc 7th Int Conf Modern Approaches in Sci, Tech & Eng, Brussels, Belgium, June 2021*, pp. 70–80.
- Armstrong A, et al. 2016. Solar park microclimate and vegetation management effects on grassland carbon cycling. Env Res Lett 11: 074016.
- Armstrong A, *et al.* 2020. Integrating environmental understanding into freshwater floatovoltaic deployment using an effects hierarchy and decision trees. *Env Res Lett* 15: 114055.
- Bax V, et al. 2023. Floating photovoltaic pilot project at the Oostvoornse lake: Assessment of the water quality effects of three different system designs. Energy Rep 9: 1415–1425.
- Benjamins S, *et al.* 2024. Potential environmental impacts of floating solar photovoltaic systems. *Renew Sust Energy Rev* 199: 114463.
- Beven K, Binley A. 1992. The future of distributed models model calibration and uncertainty prediction. *Hydr Proc* 63: 279–298.
- Boehrer B, Schultze M. 2008. Stratification of lakes. *Rev Geophys* 46: RG2005
- Chateau PA, *et al.* 2019. Mathematical modeling suggests high potential for the deployment of floating photovoltaic on fish ponds. *Sci Total Environ* 687: 654–666.
- Costa LCA, Silva GDP. 2021. Save water and energy: a technoeconomic analysis of a floating solar photovoltaic system to power a water integration project in the Brazilian semiarid. *Int J Energy Res* 45: 17924–17941.
- Environment Agency. 2018. Water quality archive. https://environment.data.gov.uk/water-quality/view/landing. Last accessed: 26/09/24.
- Exley G, et al. 2021a. Floating photovoltaics could mitigate climate change impacts on water body temperature and stratification. Solar Energy 219: 24–33.
- Exley G, *et al.* 2021b. Scientific and stakeholder evidence-based assessment: ecosystem response to floating solar photovoltaics and implications for sustainability. *Renew Sust Energy Rev* 152: 111639.
- Exley G, *et al.* 2022. Floating solar panels on reservoirs impact phytoplankton populations: A modelling experiment. *J Env Manag* 324: 116410.
- Fenocchi A, et al. 2017. Relevance of inflows on the thermodynamic structure and on the modeling of a deep subalpine lake Lake Maggiore Northern Italy/Southern Switzerland. *Limnologica* 63: 42–56.
- Findlay A. 2022. River Thames data logger above Shiplake Lock. https://dl1.findlays.net/rawdata. Last accessed: 26/09/24.
- Godinho FN, et al. 2019. Factors related to fish kill events in Mediterranean reservoirs. Water Res 158: 280–290.
- Henderson R, et al. 2008. Experiences of algae in UK waters: a treatment perspective. Water Env J 223: 184–192.
- Herlambang IF, et al. 2024. Optimizing solar potential: site potential selection for floating photovoltaics in the Sepaku Semoi dam reservoir. 8th Hydraulic Eng Int Seminar. IOP conf ser: Earth and Environmental Science 1343, p. 012022.

- Ilgen K, *et al.* 2023. The impact of floating photovoltaic power plants on lake water temperature and stratification. *Sci Rep* 13: 7932.
- Jane SF, et al. 2021. Widespread deoxygenation of temperate lakes. Nature 594: 66–70.
- Jesson DA, et al. 2010. Thermally induced strains and stresses in cast iron water distribution pipes: an experimental investigation. J Water Supply Res Tech-Aqua 594: 221–229.
- Jin Y, et al. 2023. Energy production and water savings from floating solar photovoltaics on global reservoirs. Nat Sustain 6: 865–874.
- Kraemer BM, *et al.* 2017. Global patterns in lake ecosystem responses to warming based on the temperature dependence of metabolism. *Glob Chang Biol* 235: 1881–1890.
- Liu Z, et al. 2023. Aquatic environment impacts of floating photovoltaic and implications for climate change challenges. J Env Man 346: 118851.
- Livingstone DM, Imboden DM. 1989. Annual heat-balance and equilibrium temperature of Lake Aegeri, Switzerland. *Aquat Sci* 514: 351–369.
- Lowe JA, et al. 2019. UKCP18 Science Overview Report November 2018 (Updated March 2019). UK Meteorological Office Hadley Centre.
- Markelov I, et al. 2019. Coupling water column and sediment biogeochemical dynamics: modeling internal phosphorus loading climate change responses and mitigation measures in Lake Vansjo, Norway. J Geophys Res-Biogeosci 12412: 3847–3866.
- Mathijssen D, *et al.* 2020. Potential impact of floating solar panels on water quality in reservoirs; pathogens and leaching. *Water Prac Tech* 153: 807–811.
- Miranda LE, *et al.* 2020. Reservoir fish habitats: a perspective on coping with climate change. *Rev Fish Sci Aquacult* 284: 478–498.
- Mora-Rodríguez J, *et al.* 2015. Pathogen intrusion flows in water distribution systems: according to orifice equations. *J Water Supply: Res Technology-Aqua* 648: 857–869.
- Nobre R, et al. 2024. A global study of freshwater coverage by floating photovoltaics. Solar Energy 267: 112244.
- North RP, *et al.* 2014. Long-term changes in hypoxia and soluble reactive phosphorus in the hypolimnion of a large temperate lake: consequences of a climate regime shift. *Glob Chang Biol* 20: 811–823.
- Oliveira-Pinto S, Stokkermans J. 2020. Assessment of the potential of different floating solar technologies — overview and analysis of different case studies. *Energy Conv Man* 211: 112747.
- O'Reilly CM, *et al.* 2015. Rapid and highly variable warming of lake surface waters around the globe. *Geophys Res Lett* 42: 10,773–10,781.
- Page T, et al. 2017. Constraining uncertainty and process-representation in an algal community lake model using high frequency in-lake observations. *Ecol. Model.* 357: 1–13.
- Paerl HW, Huisman J. 2009. Climate change: a catalyst for global expansion of harmful cyanobacterial blooms. *Environ Microbiol Rep* 11: 27–37.
- Prudhomme C, *et al.* 2013. Future flows hydrology: an ensemble of daily river flow and monthly groundwater levels for use for climate change impact assessment across Great Britain. *Earth Sys Sci Data* 51: 101–107.
- Rose KC, et al. 2023. Indicators of the effects of climate change on freshwater ecosystems. Climatic Change 176: 23.
- Saloranta TM, Andersen T. 2007. MyLake a multi-year lake simulation model code suitable for uncertainty and sensitivity analysis simulations. *Ecol Mod* 2071: 45–60.

- Saulnier-Talbot E, Lavoie I. 2018. Uncharted waters: the rise of human-made aquatic environments in the age of the "Anthropocene". *Anthropocene* 23: 29–42.
- Schnoor JL. 1996. Environmental modeling: fate and transport of pollutants in water air and soil. New York: John Wiley and Sons, 682p.
- Silverio NM, et al. 2018. Use of floating PV plants for coordinated operation with hydropower plants: case study of the hydroelectric plants of the Sao Francisco River basin. Energy Conv Man 171: 339–349.
- Ta T. 2019. QEII Reservoir computational fluid dynamics model for Cryptosporidium residence time. Unpublished report prepared for Thames Water.
- Taylor CJ, et al. 2007. Environmental time series analysis and forecasting with the Captain toolbox. Env Model Software 226: 797–814.
- Thackeray SJ, *et al.* 2013. Food web de-synchronization in England's largest lake: an assessment based on multiple phenological metrics. *Glob Chang Biol* 1912: 3568–3580.
- Thackeray SJ, *et al.* 2016. Phenological sensitivity to climate across taxa and trophic levels. *Nature* 535: 241–245.
- Till A, *et al.* 2019. Fish die-offs are concurrent with thermal extremes in north temperate lakes. *Nature Climate Change* 9: 637–641.

- UK Meteorological Office. 2019. MIDAS Open: UK daily weather observation data. https://catalogue.ceda.ac.uk/uuid/6ad6792f44c84c22865lb0ldl82d9d73. Last accessed: 30/09/2024.
- UK Meteorological Office Hadley Centre. 2018. UKCP18 Probabilistic Projections by UK River Basins for 1961-2100. https://catalogue.ceda.ac.uk/uuid/10538cf7a8d84e5e872883ea09a674f3/. Last accessed 30/09/2024.
- Vachon D, et al. 2019. Influence of water column stratification and mixing patterns on the fate of methane produced in deep sediments of a small eutrophic lake. Limnol Oceanogr 645: 2114–2128.
- Watson SB, et al. 2016. Biochemistry and genetics of taste- and odorproducing cyanobacteria. Harmful Algae 54: 112–127.
- Winder M, Sommer U. 2012. Phytoplankton response to a changing climate. *Hydrobiologia* 6981: 5–16.
- Woolway RI, Merchant CJ. 2019. Worldwide alteration of lake mixing regimes in response to climate change. *Nature Geosci* 124: 271–276.
- Woolway RI, et al. 2020. Global lake responses to climate change. Nature Rev Earth & Env 18: 388–403.
- Woolway RI, et al. 2021. Phenological shifts in lake stratification under climate change. Nat Commun 12: 2318.
- Young PC. 2015. Refined instrumental variable estimation: maximum likelihood optimization of a unified Box-Jenkins model. *Automatica* 52: 35–46.

Cite this article as: Exley G, Page T, Olsson F, Thackeray SJ, Chipps MJ, Armstrong A, Folkard AM. 2025. Modelling of the potential of floating photovoltaics for mitigating climate change impacts on reservoirs. *Knowl. Manag. Aquat. Ecosyst.*, 426. 26. https://doi.org/10.1051/kmae/2025021